The equilibrium crystal shape of strontium titanate: impact of donor doping

Wolfgang Rheinheimer[*] Fabian J. Altermann and Michael J. Hoffmann

[*] Corresponding author, tel. +49 721 608 47922, wolfgang.rheinheimer@kit.edu

Institute of Applied Materials – Ceramic materials and Technologies (IAM-KWT), Karlsruhe Institute of Technology (KIT), Haid-und-Neu-Str. 7, 76131 Karlsruhe, Germany

Abstract

The present study investigates the impact of point defect concentrations on the equilibrium crystal shape of strontium titanate. Therefor the shape of intergranular pores in coarse microstructures was observed. The point defect concentration was changed by donor-doping with Nb (0.2 at% - 2.4 at%). A decreasing surface energy anisotropy was found with increasing donor dopant concentration and with increasing temperature. These findings are correlated to the defect chemistry and grain growth behavior of strontium titanate.

Key words

Equilibrium crystal shape; Anisotropy; Surface energy; Strontium titanate; Point defects

Grain growth in undoped strontium titanate is known to show a remarkable anomaly as the growth rate k decreases by orders of magnitude in the temperature range of 1350 °C – 1425 °C [1-4]. This counterintuitive behavior was observed using a standard grain growth law

$$D^2 - D_0^2 = k \cdot t = 2\alpha\gamma_{GB}m \cdot t \qquad\qquad \mathbf{1}$$

with the mean grain size D, the grain size D_0 at time $t = 0$, the grain boundary energy γ_{GB}, the grain boundary mobility m, a geometric constant α close to one [5] and the grain growth rate constant $k = 2\alpha\gamma_{GB}m$, which includes the grain boundary energy and mobility [6].

Despite of vast investigation, the origin of the grain growth anomaly of strontium titanate is yet not understood in detail. While the anomaly is most likely related to an interaction of point defects and boundary motion [3, 7, 8], the importance of interfacial anisotropy (i.e. grain boundary mobility and energy) was discussed as well [1, 9, 10]. Whereas a multitude of information on both parameters is available for the undoped material, few studies investigate the impact of point defects on the interfacial energy and its anisotropy. Accordingly the present study explores the surface energy anisotropy at different donor dopant levels for the perovskite model system strontium titanate.

As in previous studies [9, 11-13], the surface energy anisotropy was approached by observing the equilibrium crystal shape. The equilibrium crystal shape (Wulff shape) reflects the minimization of surface energy of an isolated particle or void [14, 15] and directly relates to the relative surface energy and anisotropy. However, the observation of the equilibrium crystal shape is difficult due to the kinetics of equilibration. Growing or shrinking particles or voids will generally be bounded preferentially by low-mobility and not necessarily by low-

energy planes planes, and will therefore have a kinetic impact on the crystal shape [16, 17]. Discriminating between the equilibrium shape and a kinetic shape is a central problem in every study of the Wulff shape [18, 19]. Different analytical approaches to the equilibration kinetics of particles or pores have been used [19, 20], in which the most important factor for equilibration of an isolated particle or void is its size. In this study, the Wulff shape of small intragranular pores was used to measure the anisotropy of the surface energy as a function of temperature.

Small pores needed for analysis of the Wulff shape were obtained by observing overgrown pores in coarse-grained polycrystalline microstructures, which passed through a stage of rapid grain growth. Stoichiometric polycrystalline material was prepared by a mixed oxide/carbonate route based on high purity raw materials ($SrCO_3$ and TiO_2, purity of 99.95 % and 99.995 %, Sigma Aldrich Chemie GmbH, Taufkirchen, Germany). Niobium(V)oxide (Nb_2O_5, purity of 99.9 %, chemPUR GmbH, Karlsruhe, Germany) was used as donor dopant on the B-site of the perovskite lattice. Charge compensation was assumed to be electronic. The dopant concentrations were 0.2 at%, 0.6 at%, 1.2 at% and 2.4 at% with respect to the B-site of the perovskite lattice. Further details of the powder synthesis are published elsewhere [21, 22].

Samples were sintered at 1600 °C for 10 h in a batch furnace (HTK 16K, Carbolite Gero GmbH & Co. KG, Neuhausen, Germany). At this temperature coarse-grained microstructures are obtained with a multitude of intragranular pores [9, 21].

Samples were equilibrated at 1350 °C for 96 h, at 1460 °C for 55 h and at 1600 °C for 10 h in oxygen in a tube furnace (HRTV70-250, Carbolite Gero GmbH & Co. KG, Neuhausen, Germany). In a previous study, these heating times were assumed to be sufficient for the equilibration of pores in strontium titanate [9]. Samples were quenched to room temperature at ~200 K/min to minimize changes of the pore shape during cooling.

The pore shape was observed by SEM-imaging (Nova NanoSEM 450, FEI, Hillsboro, USA). The typical size of the measured pores was 0.5–2 μm (max. 3 μm at high temperatures). At each temperature at least 5 pores (typically 10) were analyzed.

To evaluate the 3D pore shape, the SEM images were compared to a calculated pore shape using the Wulff-construction for a fully faceted pore. The energies of the facets in the Wulff-construction were adjusted until the calculated shape fitted the observed shape [9]. The orientations of the facets, which form the pore shape, were obtained by both comparing their symmetry and their position in the pore shape. Further details on this procedure are published elsewhere [9].

Figs. 1, 2 and 3a–c show SEM images of pores in strontium titanate equilibrated at 1350 °C (Fig. 1), 1460 °C (Fig. 2) and 1600 °C (Fig. 3) doped with 0.2 at% (a), 1.2 at% (b) and 2.4 at% Nb (c). The reconstructed pore shapes are shown in d–f, respectively. Since the orientation of the pores is different in the SEM images, the orientation of the corresponding facets is highlighted to ease comparison between observed and reconstructed shape. The shape with 0.6 at% Nb dopant is not shown, as it is very similar to the neighboring dopant concentrations.

In general, all pores shown in Figs. 1, 2 and 3 have a similar shape: dominant facet orientations are {100}, {110} and {111}. Almost all pores show {310}-planes as well, but not at 1350°C with 1.2 at% Nb-dopant (Fig. 1b). The reason for the missing orientation in this particular case not clear. Apart from that, the dataset shows a very consistent behavior: as reported for undopted strontium titanate [9], higher temperatures result in rounder pore shapes indicating a decreasing surface energy anisotropy. As can be seen in Figs. 1, 2 and 3, the same seems to be true for increasing dopant concentrations.

All observed pores show microfacetted (corrugated) areas as highlighted in orange in Figs. 1, 2 and 3. In general, their area fraction in the pore shape increases with increasing temperature and with increasing dopant concentration. Similar effects were published for undoped strontium titanate [9] and can appear in other materials as well [23, 24]. While facetted and round areas can be part of the Wulff shape, microfacetted areas should not occur [15]. Their presence shows that there is a constraint on the pore shape [9]. In general, this constraint can be kinetic (pinning of the corner edges or metastable surface configurations) or geometric due to the existence of saddle-shaped surfaces [25] or quad junctions in the Wulff shape [26].

Independ of the cause of the microfacetted areas, we assume that there is no significant impact on the reconstructed pore shape, since for the reconstruction of each pore shape several pores were observed and the variance within this data is low (cf. Fig. 4). Accordingly the distance of the main planes in the pores ({100}, {110}, {111} and {310}) is most likely not influenced by the microfacetting. Thus the pore shapes shown in Figs. 1, 2 and 3 are assumed to be close to equilibrium.
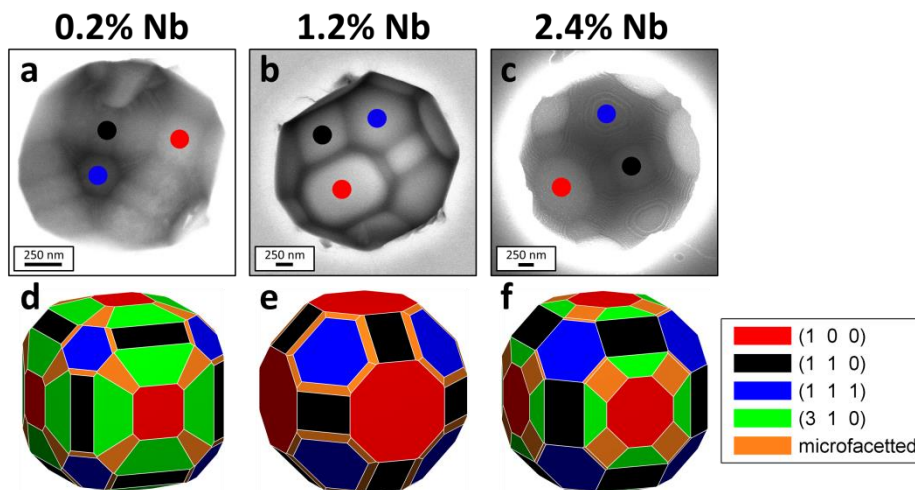

Figure 1 SEM images of pores in strontium titanate annealed at 1350°C in oxygen with 0.2 % (a), 1.2 % (b) and 2.4 % (c) Nb dopant. (d–f) Reconstructed pore shapes corresponding to a–c. Note that the orientation of pores is different in a–c. To guide the eye one facet with the orientation {100}, {110} and {111} is highlighted in a–c according to the color legend.
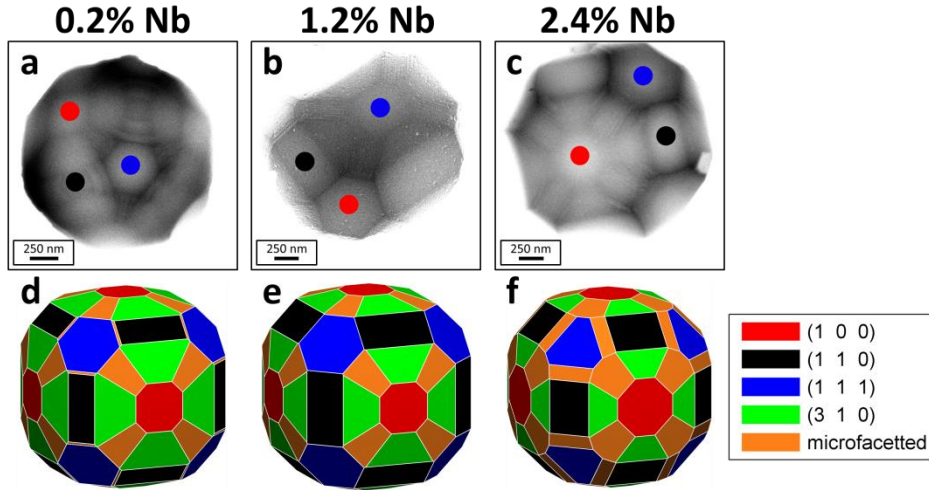
Figure 2 SEM images of pores in strontium titanate annealed at 1460°C in oxygen with 0.2 % (a), 1.2 % (b) and 2.4 % (c) Nb dopant. (d–f) Reconstructed pore shapes corresponding to a–c. Note that the orientation of pores is different in a–c. To guide the eye one facet with the orientation {100}, {110} and {111} is highlighted in a–c according to the color legend.
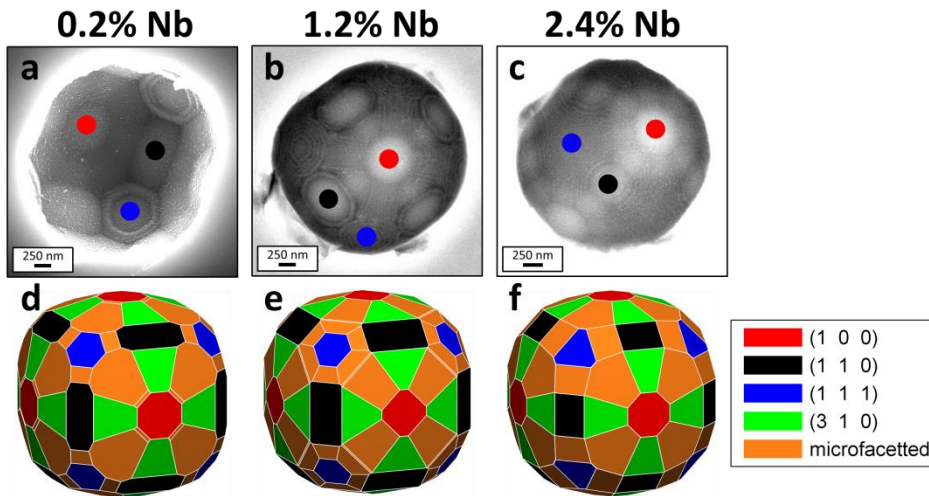

Figure 3 SEM images of pores in strontium titanate annealed at 1600°C in oxygen with 0.2 % (a), 1.2 % (b) and 2.4 % (c) Nb dopant. (d–f) Reconstructed pore shapes corresponding to a–c. Note that the orientation of pores is different in a-c. To guide the eye one facet with the orientation {100}, {110} and {111} is highlighted in a-c according to the color legend.

The Wulff theorem states that the relative surface energy of a particular facet in the Wulff shape is proportional to its distance to the center of the Wulff shape [14, 15]. Accordingly, if the Wulff shape is known, the relative surface energy of all visible facets is known. Note that this only holds for those orientations, which are included in the Wulff shape; for all other orientations only a minimum relative surface energy can be obtained ('missing orientations' [27]).

Given the reconstructed pore shapes from Figs. 1-3 and assuming that they are close to equilibrium, the relative surface energy of the four orientations {100}, {110}, {111} and {310} can be extracted. This data is shown in Fig. 4. All three datasets show a continuous decrease of the surface energy anisotropy with increasing dopant concentration. At 1350°C, the difference between highest and lowest energy orientation in the Wulff shape (i.e. {111} and {100}) decreases from 22 % to 9 %. At 1460 °C it decreases from 15% to 7% and at 1600°C from 12 % to 7 %. As with the pore shapes itself, an inconsistency can be found: at 1350°C and 1.2at % Nb {310} is missing and {111} has a very low surface energy. As expected, a comparison with Fig. 4a-c shows that the surface energy anisotropy decreases with increasing temperature as well [9].
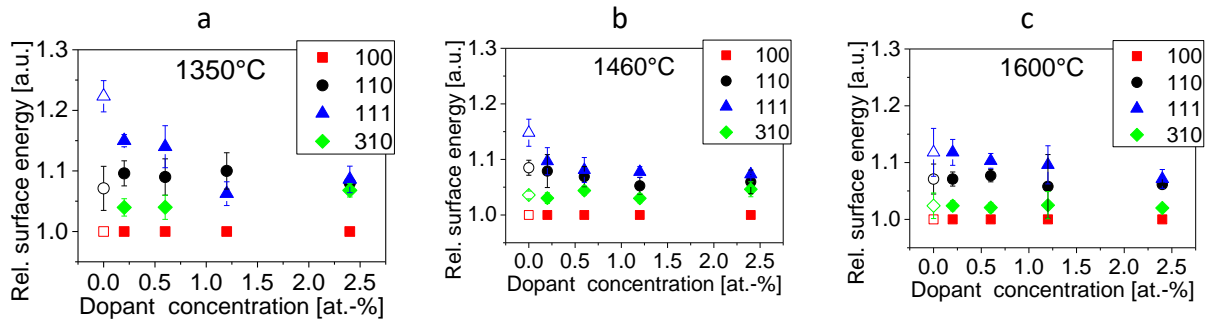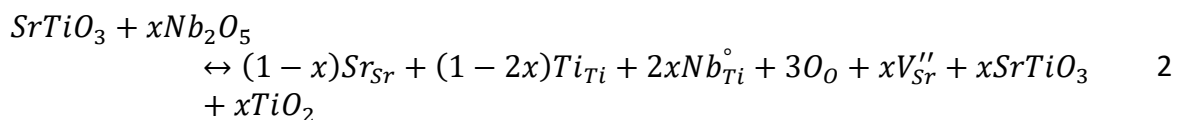

Figure 4 Relative surface energy of strontium titanate as obtained by the pore shape at 1350 °C(a), 1460 °C (b) and 1600 °C (c) in oxygen with 0.2 % – 2.4 at% Nb dopant. Open symbols show the relative surface energy for undoped strontium titanate [9].
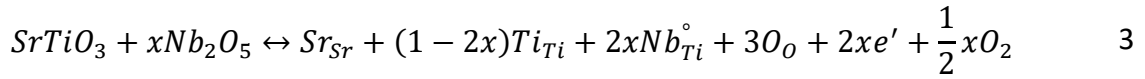
In perovskites, the segregation of donor dopants towards the grain boundaries is well known [28] and, in general, is attended (or driven) by a reduction of the interfacial energy [29]. This is to be expected from thermodynamics, since a segregation of defects should increase the entropy at the interface [29, 30]. This concept applies to surfaces as well.

While Fig. 4 does not provide information on the absolute surface energy, it has shown that the anisotropy of the surface energy decreases with both increasing temperature and increasing donor dopant concentration. According to the literature the same is true for a decreasing oxygen partial pressure as well [9]. All three parameters (donor doping, temperature and oxygen partial pressure) impact the point defect concentration. As is discussed in the following, an increase in the vacancy concentration (Sr or O vacancies) seems to result in a decreasing surface energy anisotropy.

The defect chemistry of strontium titanate delivers two different charge compensation mechanisms for donor doping [31]. First, the positive charge of the dopant can be compensated by Sr vacancies:

$$SrTiO_3 + xNb_2O_5$$
$$\leftrightarrow (1-x)Sr_{Sr} + (1-2x)Ti_{Ti} + 2xNb_{Ti}^{\circ} + 3O_O + xV_{Sr}'' + xSrTiO_3 \qquad 2$$
$$+ xTiO_2$$

Second, free electrons can be formed:

$$SrTiO_3 + xNb_2O_5 \leftrightarrow Sr_{Sr} + (1 - 2x)Ti_{Ti} + 2xNb_{Ti}^{\circ} + 3O_O + 2xe' + \frac{1}{2}xO_2 \qquad 3$$

In general electronic compensation is more important, although with increasing temperature the compensation shifts towards Sr vacancy concentration [31]. Nevertheless, we can assume that at least in parts the dopant is accommodated by Sr vacancies, since the temperatures in the presented experiments are high. Accordingly, an increasing donor dopant concentration results in an increasing Sr vacancy concentration. Following Fig. 4, this is attended by a decreasing surface energy anisotropy.

Lowering the oxygen partial pressure results in the formation of oxygen vacancies and free electrons in the material:

$$O_O \leftrightarrow V_O^{\circ\circ} + \frac{1}{2}O_2(g) + 2e' \qquad 4$$

For this case a decreasing surface energy anisotropy was reported as well [9]. A decreasing surface energy anisotropy with increasing temperature was found in the present study and is to be expected; again we can argue that a correlation to the vacancy concentration (which increases with temperature [31]) exists.

In summary, the results seem to indicate a decreasing surface energy anisotropy with increasing vacancy concertation; the species of the vacancy seems not to be important. This is most likely caused by a dependence of the surface relaxation on the vacancy concentration: a higher concentration of vacancies may provide more freedom in local charge accommodation from broken bonds at surfaces.

Several studies on grain growth on strontium titanate [32, 33] and barium titanate [34, 35] came to the same conclusion that the grain boundary energy anisotropy seems to decrease with increasing vacancy concentration; accordingly the present results are in good agreement with the literature. Alumina seems to have a similar relationship between point defects and surface energy anisotropy, since doping reduces the anisotropy as well [13, 20].

Commonly, the grain boundary energy γ_{GB} is assumed to be the sum of two surface energies γ_1 and γ_2 less the binding energy B:

$$\gamma_{GB} = \gamma_1 + \gamma_2 - B \qquad 5$$

Thus a decreasing surface energy anisotropy indicates a decreasing grain boundary energy anisotropy as well. The grain boundary energy is a central parameter in microstructural evolution. Its anisotropy plays a significant role in grain growth and microstructure morphology as it defines the dihedral angle distribution and thereby local driving force in polycrystals [36-41]. As a consequence bimodal microstructures may arise [36, 42, 43]. Interfacial anisotropy was argued to be important for the grain growth anomaly and the formation of bimodal microstructures in strontium titanate as well [1-3, 9, 10, 32]. Given the results of the present study, the impact of grain boundary anisotropy on the grain growth anomaly can be further evaluated by observing bimodal grain growth in the transition temperature regime of the grain growth anomaly with respect to donor dopant concentration.

References

[1]   Rheinheimer W, Hoffmann M. Journal of Materials Science 2015; HTC 2015:1.

[2]   Rheinheimer W, Hoffmann MJ. Scr Mater 2015; 101:68.

[3]   Rheinheimer W, Hoffmann MJ. Current Opinion in Solid State and Materials Science 2016; :.

[4]   Amaral L, Fernandes M, Reaney IM, Harmer MP, Senos AMR, Vilarinho PM. The Journal of Physical Chemistry 2013; 117:24787.

[5]   Burke JE, Turnbull D. Progress in Metal Physics 1952; 3:220.

[6]   Bäurer M, Weygand D, Gumbsch P, Hoffmann MJ. Scr Mater 2009; 61:584–587.

[7]   Sternlicht H, Rheinheimer W, Hoffmann MJ, Kaplan WD. J Mater Sci 2015; 51:467.

[8]   Bäurer M, Shih SJ, Bishop C, Harmer MP, Cockayne D, Hoffmann MJ. Acta Mater 2010; 58:290.

[9]   Rheinheimer W, Bäurer M, Chien H, Rohrer GS, Handwerker CA, Blendell JE, Hoffmann MJ. Acta Mat 2015; 82:32.

[10]   Rheinheimer W, Bäurer M, Handwerker C, Blendell J, Hoffmann M. Acta Materialia 2015; 95:111 .

[11]   Kitayama M, Glaeser A. J Am Ceram Soc 2002; 85:611.

[12]   Kim CK, Kim KH, Kuk IH, Kang SJL. Journal of Nuclear Materials 1994; 209:315 .

[13]   Choi J, Kim D, Hockey B, Wiederhorn S, Blendell J, Handwerker C. J Am Ceram Soc 2002; 85:1841.

[14]   Wulff GV. Zeitschrift für Krystallographie und Mineralogie 1901; 34:449.

[15]   Herring C. Phys Rev 1951; 82:87.

[16]   Wettlaufer JS, Jackson M, Elbaum M. Journal of Physics A - Mathematical and General 1994; 27:5957.

[17]   Sekerka RF. Cryst Res Technol 2005; 40:291. 4th International Conference on Solid State Crystals/7th Polish Conference on Crystal Growth, Zakopane Koscielisko, Poland, May 16-20, 2004.

[18]   Carter WC, Roosen AR, Cahn JW, Taylor JE. Acta Metallurgica et Materialia 1995; 43:4309.

[19]   Kern R. Morphology of crystals Part A: Fundamentals, volume A, chapter The equilibrium form of a crystal. Tokyo: Terra Scientific Publ., 1987, 77.

[20]   Choi JH, Kim DY, Hockey B, Wiederhorn S, Handwerker C, Blendell J, Carter W, Roosen A. J Am Ceram Soc 1997; 80:62.

[21]   Bäurer M, Zagonel LF, Barrett N, Hoffmann MJ. Journal of Physics: Conference Series 2008; 94:012015.

[22]   Bäurer M, Kungl H, Hoffmann MJ. J Am Ceram Soc 2009; 92:601.

[23]   Chatain D, Wynblatt P, Rohrer G. Scr Mater 2004; 50:565.

[24]   Wynblatt P, Chatain D. Reviews on Advanced Materials Science 2009; 21:44.

[25]   Taylor JE, Cahn JW. Acta Metallurgica 1986; 34:1.

[26]   Blendell JE, Carter WC, Handwerker CA. J Am Ceram Soc 1999; 82:1889.

[27]   Cahn J, Handwerker C. Materials science and engineering A-Structural materials properties microstructure and processing 1993; 162:83.

[28]   Chiang YM, Takagi T. J Am Ceram Soc 1990; 73:3278.

[29]   Sutton AP, Balluffi RW. Interfaces in crystalline materials, volume 51 of Monographs on the physics and chemistry of materials. Oxford: Clarendon Press, 1996, 1 edition.

[30]   Wynblatt P, Chatain D. METALLURGICAL AND MATERIALS TRANSACTIONS A-PHYSICAL METALLURGY AND MATERIALS SCIENCE 2006; 37A:2595.

[31]   Moos R, Härdtl K. J Am Ceram Soc 1997; 80:2549.

[32]   Chung SY, Yoon DY, Kang SJL. Acta Mater 2002; 50:3361.

[33]   Kang SJL, Chung SY, Nowotny J. Key Engineering Materials 2003; 253:63.

[34]   An SM, Kang SJL. Acta Mater 2011; 59:1964.

[35]   Fisher JG, Kang SJL. Materials Science Forum 2012; 715-716:719.

[36]   Rohrer GS. Annual Reviews 2005; 35:99.

[37]   Kazaryan A, Wang Y, Dregia SA, Patton BR. Acta Mater 2002; 50:2491.

[38]   Bäurer M, Syha M, Weygand D. Acta Mater 2013; 61:5664.

[39]   Upmanyu M, Hassold GN, Kazaryan A, Holm EA, Wang Y, Patton B, Srolovitz DJ. Interface Science 2002; 10:201.

[40]   Holm EA, Foiles SM. Science 2010; 328:1138.

[41]   Rohrer GS. J Mater Sci 2011; 46:5881.

[42]   Bojarski SA, Ma S, Lenthe W, Harmer MP, Rohrer GS. Metallurgical and Materials Transactions A-Physical Metallurgy and Materials Science 2012; 43A:3532.

[43]   Bojarski SA, Stuer M, Zhao Z, Bowen P, Rohrer GS. J Am Ceram Soc 2014; 97:622.